Metal ion and oxygen vacancies in bulk and thin film $La_{1-x}Sr_xCoO_3$

T. Friessnegg* and S. Madhukar
Department of Materials Science and Nuclear Engineering, University of Maryland, College Park, Maryland 20742

B. Nielsen and A. R. Moodenbaugh
Division of Materials Science, Brookhaven National Laboratory, Upton, New York 11973

S. Aggarwal
Department of Materials Science and Nuclear Engineering, University of Maryland, College Park, Maryland 20742

D. J. Keeble
Carnegie Laboratory of Physics, University of Dundee, Dundee DD1 4HN, United Kingdom

E. H. Poindexter
Army Research Laboratory, Adelphi, Maryland 20783

P. Mascher
Centre for Electrophotonic Materials and Devices, Department of Engineering Physics, McMaster University, Hamilton, Ontario, Canada L8S 4L7

R. Ramesh
Department of Materials Science and Nuclear Engineering, University of Maryland, College Park, Maryland 20742
(Received 30 April 1998)

Positron-lifetime and depth-resolved Doppler-broadening spectroscopy were used to investigate vacancies formed in bulk and laser ablated thin film $La_{1-x}Sr_xCoO_3$. In bulk samples, metal ion vacancies, which are most likely situated in the La sublattice, show a lifetime of 219 ps and a Doppler-broadening S parameter 1.06 times higher than the bulk. The metal-ion vacancy concentration increases with increasing Sr content. For $x \geq 0.3$, oxygen vacancies are detected, yielding a positron lifetime of 149 ps, only 10 ps longer than the bulk lifetime; the S parameter is 4% higher than for the bulk. For a given Sr concentration the films show a higher defect density than the bulk samples. The introduction of oxygen vacancy related defects is observed for increasing Sr doping concentration for both film and bulk samples. In films these defects probably consist of larger clusters and/or form complexes with metal ion vacancies. [S0163-1829(99)03519-5]

I. INTRODUCTION

Due to its high electrical and ionic conductivity, the perovskite structure $La_{1-x}Sr_xCoO_3$ is of great technological interest. It is a promising material for use as a cathode in solid oxide fuel cells,[1,2] as an oxygen permeable membrane[3] and as an electrode for highly oriented ferroelectric thin films.[4] The insulator-metal transition in $La_{1-x}Sr_xCoO_3$, which also occurs in $LaCoO_3$ at high temperature,[5,6] has attracted much attention. $La_{1-x}Sr_xCoO_3$ has low-electrical conductivity for $x=0$, is semiconductive for $0.20 \leqslant x \leqslant 0.25$, and metallic for $0.30 \leqslant x \leqslant 0.50$, respectively.[7]

When La^{3+} ions are replaced by Sr^{2+} ions, the negative effective charge of strontium ions may be compensated by the formation of equivalent amounts of positive charge. These may constitute either, formally, Co^{4+} ions or positively charged oxygen vacancies.[8] This can result in a complex defect structure with regard to oxygen nonstoichiometry and strontium content. In recent publications,[9,10] we have demonstrated that vacancy-type defects are detected in $La_{0.5}Sr_{0.5}CoO_{3-\delta}$ thin films by positrons where the oxygen deficiency δ was altered by varying the oxygen partial pressure during cooling. In this paper, we employ the vacancy sensitive technique of positron annihilation spectroscopy on both bulk and thin films of $La_{1-x}Sr_xCoO_3$ to investigate the defect structures. By combining positron-lifetime spectroscopy on bulk samples with variable energy positron beam Doppler-broadening on laser ablated thin films, metal ion vacancies and oxygen vacancy-related defects are directly observed.

II. EXPERIMENTAL DETAILS

Bulk polycrystalline samples were prepared by a solid-state reaction method similar to that described by Itoh *et al.*[11] Appropriate mixtures of La_2O_3, $SrCO_3$, and $CoCO_3$ were ground together. The powders were placed into alumina boats and calcined in air at 950 °C for 16 h, then reground and sintered 16 h at 1000 °C, then again for 16 h at 1100 °C. Pellets were pressed, then placed onto alumina plates, and fired in air for 12 h at 1300 °C. Finally, the samples were annealed in flowing oxygen, being heated 500 °C/h to 1000 °C, held 1 h, then cooled at ~6 °C/h to below 100 °C. Powder x-ray diffraction analysis confirmed that the samples

are single phase with rhombohedrally distorted perovskite structure. Electrical characterization of similarly prepared samples showed that the material exhibits a crossover from semiconducting to metallic close to $x=0.25$.[12]

Thin films of $La_{1-x}Sr_xCoO_3$ were grown on $LaAlO_3$ substrates by pulsed excimer laser deposition using a solid ceramic target of the desired film composition. During deposition, a temperature of 650 °C and a pressure of 100 mTorr oxygen were maintained in the growth chamber. After growth, the films were cooled at 5°/min in an oxygen pressure of 760 Torr. The phase purity and structural quality of the films was evaluated by x-ray diffraction, showing epitaxial films with a (001) orientation. The film thicknesses were between 250 and 500 nm as determined by Rutherford backscattering.

Two experimental positron-based techniques were employed to characterize the defect structure of bulk and thin film $La_{1-x}Sr_xCoO_3$. The sensitivity of these techniques to open volume defects arises from the annihilation characteristics of the thermalized positron with the electrons in the investigated material.[13,14] Positrons are attracted to vacancy-type defects because of the missing ion cores and can, therefore, be trapped by these defects. This results in a significant change in the annihilation characteristics that can be used to investigate defect chemistry.

Positron-lifetime spectroscopy was performed on bulk $La_{1-x}Sr_xCoO_3$ using a lifetime spectrometer with a time-resolution full width at half-maximum (FWHM) of 220 ps. The positron source was a 30 μCi ^{22}NaCl source encapsulated in an Al foil with a thickness of (2.4 ± 0.2) μm. The fraction of positrons annihilating in the source was determined by a method described elsewhere[15] to a total of $(4.3\pm0.4)\%$. A correction was made for this source contribution to the annihilation spectrum. The computer program PATFIT-88 (Ref. 16) was used for analyzing the lifetime spectra. To accurately resolve the lifetimes $\sim 6\times10^6$ counts were accumulated in each spectrum.

The lifetime spectra were analyzed with three lifetime components yielding χ^2 values for the fit of typically less than 1.1 (A fit with two lifetime components gave $\chi^2>2.0$ indicating an inappropriate decomposition of the lifetime spectra). A long lifetime $(1.1\pm0.1\,\text{ns})$ component with an intensity $<1\%$ of the total was present in all samples. This small component, which is attributed to annihilations at the surfaces and in the ^{22}Na source, was fixed in the analysis and will not be discussed in further detail.

Since the electron density is lower in open-volume defects, the corresponding positron lifetime is longer than that for the bulk state. The annihilations from different states can be separated by positron-lifetime spectroscopy since each state is represented by a characteristic lifetime, which can be determined by decomposition of the measured lifetime spectrum.

A variable energy positron beam[17] was used to study the defect depth profile in the bulk and thin films. The annihilation quanta were measured using a 35% efficient Ge detector with a resolution of 1.5 keV (FWHM) at 511 keV. About 5×10^5 counts were accumulated in each spectrum. The Doppler broadening of the annihilation line was analyzed in terms of the *S* parameter, defined as the ratio of the integral over a fixed central portion of the peak (*A*, 510.3–511.7 keV) and the total counts (*B*, 503.8–518.2 keV) according to $S=A/B$ (which yields a value of $\sim$0.500 for defect-free silicon).

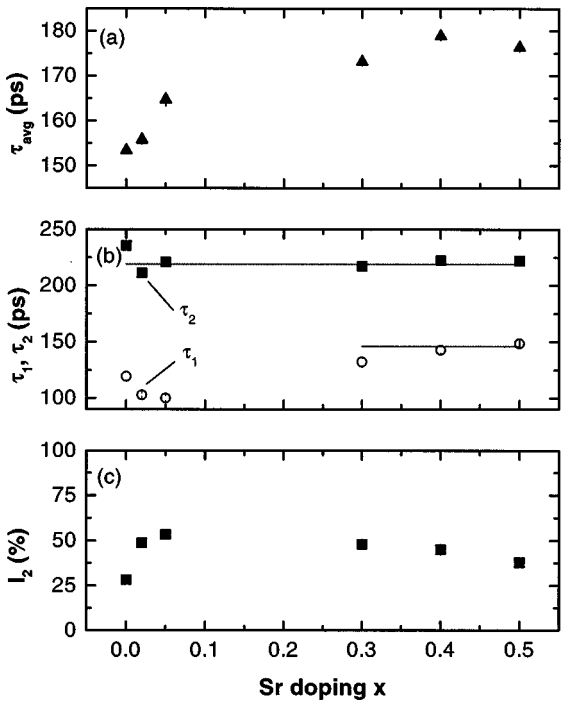

FIG. 1. Lifetime and Doppler-broadening data for bulk $La_{1-x}Sr_xCoO_3$ as a function of Sr content. (a) Doppler-broadening *S* parameter, (b) average lifetime τ_{avg}, (c) decomposed lifetimes τ_1 (open circles), τ_2 (solid squares), and (d) corresponding intensity I_2.

When a positron annihilates with an electron, the center of mass of the electron-positron pair will have a momentum that is essentially determined by the electron since the thermalized positron has a negligible momentum. This effect causes a Doppler broadening of the annihilation line. In a vacancy defect the overlap of the positrons with core electrons is reduced. Therefore, the width of the Doppler spectrum is significantly narrower for a material with defects than for the defect-free material.

III. RESULTS AND DISCUSSION

A. Bulk ceramics

Figure 1 shows the lifetime results for bulk samples with varying Sr content. The average lifetime [panel (a)], defined as

$$\tau_{avg}=I_1\tau_1+I_2\tau_2, \tag{1}$$

is calculated from the decomposed lifetimes τ_1,τ_2, and their corresponding intensities I_1 and I_2, respectively with $I_1+I_2=100\%$. The Doppler-broadening *S* parameter data for the same samples are shown in Fig. 2 [panel (a)]. These values were obtained by averaging the *S*-parameter values for positron implantation energies from 10 to 25 keV. The average lifetime and the *S* parameter both increase with Sr doping concentration, indicating an increase in the defect density, and show saturation at 0.30 Sr doping.

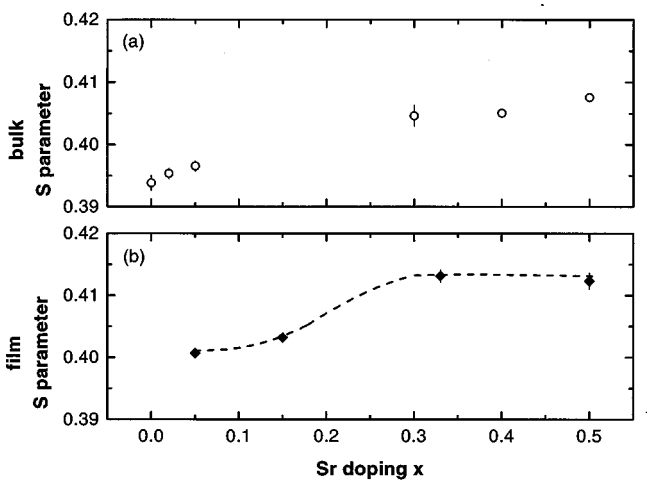

FIG. 2. *S* parameter as a function of Sr content for the bulk and laser-ablated film material. The *S* parameters were extracted from averaging the *S* values for implantation energies in (a) bulk samples for $10\,\mathrm{keV} \leqslant E \leqslant 25\,\mathrm{keV}$ and (b) film samples for $5\,\mathrm{keV} \leqslant E \leqslant 10\,\mathrm{keV}$.

From the decomposed lifetime data a longer lifetime τ_2 is resolved and can be attributed to annihilations in a vacancy-type defect. This lifetime has an average value of (219 ± 5) ps and is slightly higher for the undoped sample. The increase in the intensity of the defect component I_2 [Fig. 1, panel (c)] in combination with the decrease in the lifetime τ_1 for $0 \leqslant x \leqslant 0.05$ Sr doping indicates an increase in the rate (λ_1) by which positrons are removed from the bulk state due to trapping according to

$$\lambda_1 = 1/\tau_1 = \lambda_{\mathrm{bulk}} + \kappa_{219}, \tag{2}$$

where λ_{bulk} denotes the bulk annihilation rate and κ_{219} the trapping rate into the defect with the lifetime $\tau_2 = 219$ ps. The trapping rate is directly proportional to the defect concentration C and follows the relation

$$\kappa_{219} = \mu C \tag{3}$$

with μ being the specific trapping rate for the defect. At sufficiently high-defect concentrations essentially all positrons become trapped by defects, and the bulk-related lifetime can no longer be resolved (this is called complete trapping). For $x \geqslant 0.3$ a new defect lifetime is resolved and due to the high trapping rate into the defects, the bulk-related lifetime can no longer be resolved.

From $0 \leqslant x \leqslant 0.05$ Sr doping, the bulk lifetime (τ_{bulk}), which represents a materials constant, can be obtained according to the standard trapping model[18]

$$\lambda_{\mathrm{bulk}} = 1/\tau_{\mathrm{bulk}} = (I_1/\tau_1 + I_2/\tau_2) \tag{4}$$

yielding $\tau_{\mathrm{bulk}} = 139 \pm 2$ ps. The derived τ_{bulk} values for different Sr doping are listed in Table I. We note that Sr doping does not change the bulk lifetime perceptibly in our samples. This observation confirms the presence of only one type of defect. Therefore, the trapping rates κ_{219} into this defect can be calculated by

$$\kappa_2 = I_2(1/\tau_1 - 1/\tau_2). \tag{5}$$

TABLE I. Bulk lifetime τ_{bulk}, trapping rate κ_{219} and fraction f of positrons trapped into the observed defect calculated from Eqs. (4), (5), and (7) for different Sr-doping levels x.

Sr x	τ_{bulk} (ps)	κ_{219} (ns^{-1})	f
0.00	138 ± 1	1.2 ± 0.1	0.14 ± 0.01
0.02	137 ± 1	2.4 ± 0.1	0.26 ± 0.01
0.05	141 ± 2	2.9 ± 0.2	0.32 ± 0.02

The lifetime data can be combined with the Doppler-broadening *S* parameter data to establish defect-specific *S* parameter values. The *S* parameter can be expressed as a sum of contributions from the bulk and from defects. In the range between $0 \leqslant x \leqslant 0.05$ Sr, *S* can be expressed as

$$S = (1-f)S_{\mathrm{bulk}} + fS_{219}, \tag{6}$$

where f represents the fraction of trapped positrons and is given by

$$f = \frac{\kappa_{219}}{\lambda_{\mathrm{bulk}} + \kappa_{219}}. \tag{7}$$

Table I lists the calculated bulk lifetimes, trapping rates, and trapped fractions for $0 \leqslant x \leqslant 0.05$ Sr doping. Since the *S* parameter and f values are experimentally known for the $x = 0.02$ and the $x = 0.05$-doped sample we have two equations to determine S_{bulk} and S_{219}. We find $S_{\mathrm{bulk}} = 0.3890 \pm 0.0025$ and $S_{219} = 0.4130 \pm 0.0030$ for these characteristic *S* parameters. Hence, the *S* parameter for the 219 ps defect is about 6% larger than the bulk value.

For the Sr doping concentrations $x \geqslant 0.30$ both the Doppler-broadening *S* parameter and the average lifetime saturate. These observations are consistent with complete trapping into defects. A new lifetime of 149 ± 4 ps is observed in addition to the 219 ps component.

Using Eq. (4) to calculate the bulk lifetime from the decomposed lifetime data yields a value of 170 ps. This is significantly too high to be accounted for by Sr doping. We therefore conclude that the 149 ps lifetime component is in fact a defect lifetime and the bulk lifetime cannot be calculated from Eq. (4) due to complete trapping. In this case, the Doppler-broadening *S* parameter contains only contributions from the defect specific *S* parameters. We, therefore, can express *S* as a weighted sum of S_{149} and S_{219}:

$$S = I_1 S_{149} + I_2 S_{219} \tag{8}$$

with the relative intensities I_1 and I_2 for the 149 ps and 219 ps components, respectively. Using the observed intensities for the $x = 0.50$ Sr-doped sample together with the given value for S_{219} we solve Eq. (8) for the defect-specific *S* parameter associated with the 149 ps lifetime component. We obtain $S_{149} = 0.4040 \pm 0.0030$, which is about 4% higher than the bulk value. It is interesting to note that the lifetime of this defect is only 10 ps higher than the bulk lifetime, but *it* gives a significant contribution to the measured *S* parameter.

The most likely physical interpretation for the 149 ps defect is that *it is due to* oxygen vacancies. Theoretical calculations for positron states in $La_{1-x}Sr_xCoO_3$ have not been done. However, such calculations do exist for the layered

perovskite superconductors $La_{2-x}Sr_xCuO_4$ (Ref. 19) and $YBa_2Cu_3O_7$ (Refs. 19 and 20). A weak-positron binding energy ($E_b=60$ meV) to single-oxygen vacancies was found in both superconductor materials exhibiting lifetimes that are very close to the positron bulk lifetime. In $YBa_2Cu_3O_7$, the binding energy increases by almost a factor of 4 for a cluster size of 4 oxygen vacancies whereas the lifetime increases by only 15 ps.[20]

The lifetime associated with oxygen vacancies is not observed in samples with $0\leqslant x\leqslant 0.05$ Sr doping. This suggests that the charge compensation for substitution of La by Sr is accomplished by oxidation of Co^{3+} to Co^{4+} in this range of Sr doping. It was reported that the concentration of Co^{4+} increases approximately linearly with Sr content up to $x=0.30$ Sr doping.[8] For higher Sr-doping concentrations the concentration of Co^{4+} was found to increase sublinearly[21] or to decrease.[8] Moreover, abrupt changes in the Co-O bond length and the Co-O-Co angle have been observed at $x\sim 0.25$ doping[21] and were attributed to a change in the band structure at the transition from semiconducting to metallic. Señarís-Rodríguez and Goodenough[7] determined that as-prepared samples with Sr content $x\leqslant 0.25$ are stoichiometric in oxygen while samples with $x>0.25$ are oxygen deficient. Because of these observations we rule out the possibility that the 149 ps lifetime is due to Co vacancies, although they would probably yield a comparable lifetime. According to a simple ionic model the local charge of the oxygen vacancy (V_O) should be $+2$. However, the charge of the V_O could be locally compensated by the association of the vacancy with two neighboring Sr ions, explaining why positrons can be trapped in these vacancies.

We now turn to the discussion of the 219 ps lifetime component. Theoretical calculations for $La_{2-x}Sr_xCuO_4$ and $YBa_2Cu_3O_7$ indicate that metal ion monovacancies can be strong positron traps ($E_b\sim 1$ eV) yielding substantially longer lifetimes than the oxygen vacancy.[19] In this light, the 219 ps lifetime component can be attributed to metal ion vacancies. It is worth noting that the calculated lifetime for La monovacancies in $La_{2-x}Sr_xCuO_4$ is 238 ps.[19] Considering the similar atomic composition of $La_{2-x}Sr_xCuO_4$ and $La_{1-x}Sr_xCoO_3$ as well as the comparable ionic radii for Co and Cu, we tentatively attribute $\tau_2=219$ ps to the La monovacancy. Their concentration can be estimated by using the specific trapping coefficient for monovacancies in metals ($\mu_{IV}=10^{14}$–$10^{15}\,s^{-1}$ at) (Ref. 22) in Eq. (4) to be about 10^{-5} at. Upon Sr doping the trapping rate into these vacancies shows a 2.5-fold increase as x increases from 0.0 to 0.05 (Table I), commensurate with a 2.5-fold increase in defect concentration. For Sr doping of $x\geqslant 0.3$ absolute values for the trapping rates cannot be calculated due to saturation trapping. A lower limit for the total trapping rate (V_O and V_{La}) can be estimated if we consider a trapped fraction larger than $f=0.90$ as saturation trapping [Eq. (7)]. This yields a total trapping rate of 72 ns^{-1}, which exhibits a larger than 60-fold increase in defect concentration compared to the undoped sample.

B. Films

Figure 3 shows the S parameter for $La_{1-x}Sr_xCoO_3$ on $LaAlO_3$ substrates with $0.05\leqslant x\leqslant 0.50$ as a function of incident positron energy. Three main features are visible in both S parameter profiles. At shallow implantation depths a higher S parameter arises from annihilations in the near surface region. Positrons implanted with energies up to approximately 12 keV annihilate predominantly in the deposited film. At higher energies positrons will probe both the $La_{1-x}Sr_xCoO_3$ film and the $LaAlO_3$ substrate, since the energy width of the implantation profile (FWHM) scales with the implantation energy. The resulting S therefore contains contributions from both film and substrate. Figure 2(b) shows the S parameter in the $La_{1-x}Sr_xCoO_3$ films as a function of Sr doping, which was extracted by averaging the S values for implantation energies $5\,\text{keV}\leqslant E\leqslant 10$ keV.

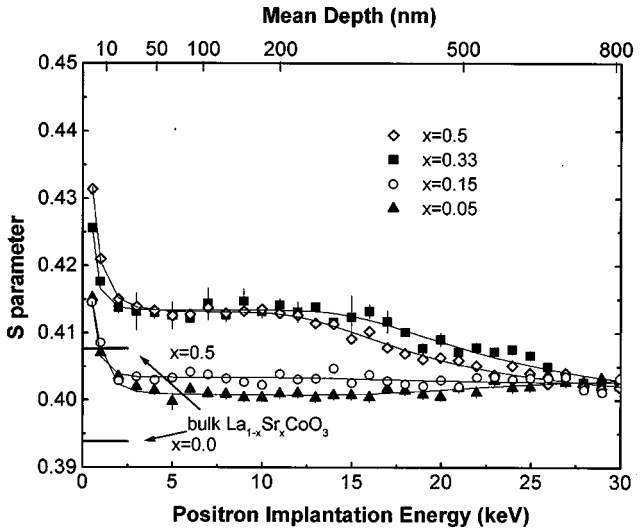

FIG. 3. S parameter as a function of incident positron energy for laser-ablated $La_{1-x}Sr_xCoO_3$ thin films for different Sr content. The lines are a guide to the eye. For comparison the S parameters for bulk samples with $x=0$ and $x=0.50$ Sr-doping concentration are also shown.

S-parameter data for the bulk samples is presented in Fig. 2(a). Both film and bulk material show similar systematic trends as a function of Sr doping: The S parameter increases by about 3% between $x=0.05$ and $x=0.3$ and saturates for higher Sr-doping concentrations. For the same nominal composition the film S parameter is higher than that of the bulk sample, indicating a larger defect density in the films. Since the same systematic trends are observed in bulk and film samples, we feel that at a given Sr-doping level, the type of defects present in films is similar to that of the bulk. In this picture, the higher S values at a given composition for the film is accounted for by a higher defect concentration. Under this assumption, we can use the defect characteristic S parameters established for the bulk samples to estimate defect concentrations in the $x=0.05$ Sr-doped film. With the given values for S_{bulk}, S_{219}, λ_{bulk}, and the measured S we can solve Eqs. (6) and (7) for the trapping rate

$$\kappa_{219}=\lambda_{bulk}\frac{S-S_{bulk}}{S_{219}-S}. \tag{9}$$

This yields a trapping rate of 6.4 ns^{-1} for the La vacancy and represents a 2.2-fold increase in defect concentration compared to the bulk sample with the same composition. The increase in S with Sr doping at $x\sim 0.3$ is comparable to that

observed in bulk samples. In the bulk samples, this was attributed to the formation of oxygen vacancies. In the film, however, the measured S value is clearly higher than that for oxygen vacancies. Nevertheless, we believe that the increase in S for $x \geq 0.3$ is most likely due to oxygen related defects, probably including larger oxygen vacancy complexes, yielding a defect-specific S parameter, which is expected to be larger than the calibrated S_{149}. A marked increase in S, observed for films grown with low-oxygen partial pressures[9,10] (yielding oxygen deficiency), suggests that oxygen vacancy clusters can be formed. At this point we cannot rule out the possibility that oxygen vacancies form complexes with La vacancies, which would also result in a larger defect-specific S.

IV. CONCLUSION

A comprehensive study of the defect structure in $La_{1-x}Sr_xCoO_3$ with $0 \leq x \leq 0.5$ has been performed. Positron-lifetime and Doppler-broadening investigations on bulk and laser ablated thin-film material have shown the following.

(a) Metal ion vacancies were found to be present in the bulk material in the entire composition range studied. These vacancies are probably situated on the La sublattice. Their concentration was found to increase with Sr doping.

(b) Oxygen vacancies become observable in both bulk and film material for $x \geq 0.3$. These vacancies are probably larger clusters, which may form complexes with metal ion vacancies in the film samples.

(c) Film samples show generally a higher defect density throughout the composition range studied than the corresponding bulk material.

ACKNOWLEDGMENTS

This work was supported by the Army Research Laboratory under Contract No. DAAL01-95-2-3530 and by the Department of Energy, the Office of Basic Energy Sciences, Division of Materials Science under Contract No. DE-AC02-98CH10886. In Canada, this work has been supported by the Natural Science and Engineering Research Council.

*Present address: Department of Applied Science, Materials Science Division Bldg. 480, Brookhaven National Laboratory, Upton, NY 11973-5000. Electronic address: friessn@bnl.gov

[1] J. B. Goodenough and R. C. Raccah, J. Appl. Phys. **36**, 1031 (1963).

[2] Y. Kaga, Y. Ohno, K. Tsukamoto, F. Uchiyama, M. J. Lain, and T. Nakajima, Solid State Ionics **40/41**, 1000 (1990).

[3] Y. Teraoka, H. Zhang, S. Furukawa, and N. Yamazoe (unpublished).

[4] R. Ramesh, H. Gilchrist, T. Sands, V. G. Keramidas, R. Haakenaasen, and D. K. Fork, Appl. Phys. Lett. **63**, 3592 (1993).

[5] J. B. Torrance, P. Lacorre, C. Asavaroengchai, and R. M. Metzger, Physica C **182**, 351 (1991).

[6] A. Chainani, M. Matthew, and D. D. Sarma, Phys. Rev. B **46**, 9976 (1992).

[7] M. A. Señarís-Rodríguez and J. B. Goodenough, J. Solid State Chem. **118**, 323 (1995).

[8] A. N. Petrov, O. F. Kononchuk, A. V. Andreev, V. A. Cherepanov, and P. Kofstad, Solid State Ionics **80**, 189 (1995).

[9] S. Madhukar, S. Aggarwal, A. M. Dhote, R. Ramesh, D. Keeble, and E. Poindexter, J. Appl. Phys. **81**, 3543 (1997).

[10] D. J. Keeble, A. Krishnan, T. Friessnegg, B. Nielsen, S. Madhukar, S. Aggarwal, R. Ramesh, and E. H. Poindexter (unpublished).

[11] M. Itoh, I. Natori, S. Kubota, and K. Motoya, J. Phys. Soc. Jpn. **63**, 1486 (1994).

[12] V. Golovanov, L. Mihaly, and A. R. Moodenbaugh, Phys. Rev. B **53**, 8207 (1996).

[13] *Positron Solid-State Physics*, Proceedings of the International School of Physics ''Enrico Fermi,'' Varena, 1981, edited by W. Brandt and A. Dupasquier (North-Holland, Amsterdam, 1983).

[14] *Positron Spectroscopy of Solids*, Proceedings of the International School of Physics ''Enrico Fermi,'' Varena, 1993, edited by A. Dupasquier and A. P. Mills, Jr. (IOS, Ohmsha, 1995).

[15] J. Mahony, T. Friessnegg, G. Tessaro, P. Mascher, and W. Puff, Appl. Phys. A: Mater. Sci. Process. **63A**, 299 (1996).

[16] P. Kirkegaard, N. J. Pedersen, and M. Eldrup, *PATFIT-88: A Data-Processing System for Positron Annihilation Spectra on Mainframe and Personal Computers* (RisØ National Laboratory, Denmark, 1989).

[17] K. G. Lynn, B. Nielsen, and T. H. Quateman, Appl. Phys. Lett. **47**, 239 (1985).

[18] R. N. West, Adv. Phys. **22**, 263 (1973).

[19] T. McMullen, P. Jena, S. N. Khanna, Yi Li, and K. O. Jensen, Phys. Rev. B **43**, 10 422 (1991).

[20] S. Ishibashi, R. Yamamoto, M. Doyama, and T. Matsumoto, J. Phys.: Condens. Matter **3**, 9169 (1991).

[21] A. Mineshige, M. Inaba, T. Yao, Z. Ogumi, K. Kikuchi, and M. Kawase, J. Solid State Chem. **121**, 423 (1996).

[22] R. M. Nieminen and J. Laakkonen, Appl. Phys. **20**, 181 (1979).